Breakdown of the Law of Reflection at a Disordered Graphene Edge

Walter, E.; Rosdahl, T. O.; Akhmerov, A. R.; Hassler, F.

DOI
10.1103/PhysRevLett.121.136803

Publication date
2018

Document Version
Final published version

Published in
Physical Review Letters

Breakdown of the Law of Reflection at a Disordered Graphene Edge

E. Walter,[1,2,*] T. Ö. Rosdahl,[3,†] A. R. Akhmerov,[3] and F. Hassler[1]
[1]JARA Institute for Quantum Information, RWTH Aachen University, 52056 Aachen, Germany
[2]Arnold Sommerfeld Center for Theoretical Physics, Ludwig-Maximilians-University Munich, 80333 Munich, Germany
[3]Kavli Institute of Nanoscience, Delft University of Technology, P.O. Box 4056, 2600 GA Delft, Netherlands

(Received 20 April 2018; revised manuscript received 24 August 2018; published 25 September 2018)

The law of reflection states that smooth surfaces reflect waves specularly, thereby acting as a mirror. This law is insensitive to disorder as long as its length scale is smaller than the wavelength. Monolayer graphene exhibits a linear dispersion at low energies and consequently a diverging Fermi wavelength. We present proof that for a disordered graphene boundary, resonant scattering off disordered edge modes results in diffusive electron reflection even when the electron wavelength is much longer than the disorder correlation length. Using numerical quantum transport simulations, we demonstrate that this phenomenon can be observed as a nonlocal conductance dip in a magnetic focusing experiment.

DOI: 10.1103/PhysRevLett.121.136803

Introduction.—The law of reflection is a basic physical phenomenon in geometric optics. As long as the surface of a mirror is flat on the scale of the wavelength, a mirror reflects incoming waves specularly. In the opposite limit when the surface is rough, reflection is diffusive and an incident wave scatters into a combination of many reflected waves with different angles. This picture applies to all kinds of wave reflection, including sound waves and particle waves in quantum systems. The phenomenon has been extensively investigated both theoretically and experimentally in the past, e.g., in order to understand sea clutter in radar [1] as well as a method to measure surface roughness [2].

Graphene [3,4] is a gapless semiconductor with a linear dispersion relation near the charge neutrality point, and therefore a diverging Fermi wavelength. Modern techniques allow for the creation of graphene monolayers of high mobility, with mean free paths of tens of microns [5–8]. This makes it possible to realize devices in which carriers propagate ballistically over mesoscopic distances, facilitating the design of electron optics experiments [9–11]. For example, recent experiments employ perpendicular magnetic fields to demonstrate snaking trajectories in graphene p-n junctions [12,13], or the magnetic focusing of carriers through cyclotron motion [14]. The latter tests the classical skipping orbit picture of carrier propagation along a boundary [15], and using a collimator to focus a narrow beam of electrons with a small angular spread enhances the focusing resolution [16]. The high mobility in the bulk together with a large Fermi wavelength suggest that graphene is a promising medium for the design of advanced electron optics and testing the law of reflection, cf. Fig. 1.

Graphene edges are rough due to imperfect lattice termination or hydrogen passivation of dangling bonds [17,18]. Boundary roughness may adversely affect device performance [19–22]. On the other hand, close to the charge neutrality point the Fermi wavelength in graphene diverges, and by analogy with optics, one may expect that the law of reflection holds and suppresses the diffusive boundary scattering.

In this Letter, we study how the microscopic boundary properties influence electron reflection off a graphene boundary. Most boundaries result in the self-averaging of the boundary disorder, and therefore obey the law of reflection. However, we find that, due to resonant scattering, electrons are reflected diffusively regardless of the Fermi wavelength when the disorder-broadened edge states overlap with $E = 0$. As a result, in this situation, the boundary of graphene never acts as a mirror and thus breaks the law of reflection. We demonstrate that this phenomenon can be observed as a dip in the nonlocal conductance in a magnetic focusing setup (see Fig. 1). We confirm our predictions by numerical simulations.

Reflection at a disordered boundary.—To demonstrate the breakdown of the law of reflection, we first analyze scattering at the edge of a semi-infinite graphene sheet. We consider a zigzag edge, since the zigzag boundary condition applies to generic lattice terminations [23]. To begin with, we neglect intervalley scattering to simplify the analytical derivation, and focus on the single valley Dirac Hamiltonian

$$H = v_F \boldsymbol{\sigma} \cdot \boldsymbol{p}, \tag{1}$$

with v_F the Fermi velocity, $\boldsymbol{\sigma} = (\sigma_x, \sigma_y)^T$ the vector of Pauli matrices in the (sublattice) pseudospin space, and $\boldsymbol{p}$ the momentum. We later verify the validity of our conclusions with tight-binding calculations that include intervalley scattering. We introduce edge disorder by randomly

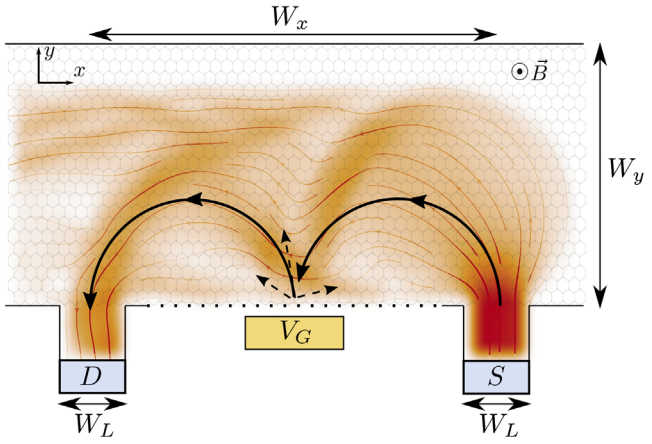

FIG. 1. Sketch of the setup. Electrons injected at the source (S) follow cyclotron trajectories due to the perpendicular magnetic field $\boldsymbol{B} = B\hat{z}$, forming a hot spot at the boundary where most trajectories scatter. If the trajectories specularly reflect at the boundary and the separation W_x between the midpoints of the source and the drain (D) matches two cyclotron diameters, most trajectories enter the drain, and a focusing peak manifests in the nonlocal conductance. The focusing is evident in the classical cyclotron trajectory of an electron normally incident from S at the Fermi level (solid curves), and in the computed current distribution that is superimposed on the device (flow lines, colored background). A side gate V_G controls the average potential at the disordered boundary (dotted line), and allows us to tune between regimes of specular and diffusive reflection (see main text). In the diffusive regime, electrons scatter into random angles as shown schematically with the dashed lines, resulting in a drop in the focusing peak conductance compared to the regime of specular reflection. The graphene sheet is grounded, such that current due to off-resonance trajectories may drain away to the sides (open boundaries).

sampling the most general single-valley boundary condition [23–25] over the edge, such that the boundary condition for the wave function reads

$$\psi(x, y = 0) = [\cos\theta(x)\sigma_z + \sin\theta(x)\sigma_x]\psi(x, y = 0), \quad (2)$$

where disorder enters through the position-dependent parameter θ, and $\theta = 0$ gives a zigzag segment. We take $\theta(x)$ to follow a Gaussian distribution with mean value $E[\theta(x)] = \theta_0$ and covariance $\mathrm{Cov}[\theta(x), \theta(x')] = s_\theta^2 e^{-\pi(x-x')^2/d^2}$, with d the correlation length. In this work, $E[A]$ is the statistical average of A over the disordered boundary, and the corresponding variance $\mathrm{Var}(A)$. The boundary condition (2) applies to different microscopic origins of disorder, such as hydrogen passivation of dangling bonds [23] or edge reconstruction [26].

To solve the scattering problem, we introduce periodic boundary conditions parallel to the boundary with period L, such that the momentum $k_\parallel \in \{2\pi n/L | n \in \mathbb{Z}\}$ is conserved. At the Fermi energy E_F, the disordered boundary scatters an incident mode $\psi_{k_\parallel}^{\mathrm{in}}$ into the outgoing modes $\psi_{k'_\parallel}^{\mathrm{out}}$. The scattering state is

$$\psi_{k_\parallel} = \psi_{k_\parallel}^{\mathrm{in}} + \sum_{k'_\parallel} \psi_{k'_\parallel}^{\mathrm{out}} S_{k'_\parallel k_\parallel}, \quad (3)$$

where modes with $k_\parallel > k_F$ are evanescent but others propagating, with k_F the Fermi momentum, and $S_{k'_\parallel k_\parallel}$ the reflection amplitudes. An outgoing propagating mode moves away from the edge at the angle $\varphi_{k_\parallel} = \arctan(v_\parallel / v_\perp)$ relative to the boundary normal, with $v_\parallel$ and $v_\perp$ the velocities along and perpendicular to the boundary. For the incident propagating mode at $k_\parallel$, the quantum mechanical average reflection angle is therefore

$$\langle \varphi_{k_\parallel} \rangle = \sum_{k'_\parallel} \varphi_{k'_\parallel} |S_{k'_\parallel k_\parallel}|^2, \quad (4)$$

where the sum is limited to propagating modes, and $|S_{k'_\parallel k_\parallel}|^2$ is the reflection probability into the outgoing mode at $k'_\parallel$. An incident mode reflects specularly if $S_{k'_\parallel k_\parallel} = \delta_{k'_\parallel k_\parallel}$, but diffusively if it scatters into multiple angles, and the variance $\sigma^2(\varphi_{k_\parallel})$ is therefore finite for the latter. If N modes are incident, diffusiveness manifests in a finite mode-averaged variance $\sigma^2(\varphi) = \sum_{k_\parallel} \sigma^2(\varphi_{k_\parallel})/N$, or its statistical average $E[\sigma^2(\varphi)]$ over the disordered boundary. If $\lambda_F \ll L$, then $\sigma^2(\varphi)$ automatically includes the statistical average $E[\sigma^2(\varphi)]$, because the incident waves sample multiple different segments of the boundary within each period.

The scattering problem simplifies at the charge neutrality point $E_F = 0$, where only two propagating modes are active, one incident and one outgoing, both with $k_\parallel = 0$. The scattering matrix relating the propagating modes is therefore a phase factor $e^{i\phi}$, with ϕ the scattering phase, and the quantum mechanical averages of the preceding paragraph are not necessary. We expect diffusiveness to manifest as a finite variance $\mathrm{Var}(\phi)$, and have verified this numerically. To compute ϕ, we impose the boundary condition (2) on the scattering state (3).

If θ_0 is nonzero and $s_\theta \ll \theta_0$, ϕ follows a Gaussian distribution [27] with the mean

$$E[\phi] \overset{L \gg d}{=} -\theta_0 + \frac{s_\theta^2}{2\sin(\theta_0)} + \mathcal{O}\left(\frac{s_\theta^3}{\theta_0^3}\right) \quad (5)$$

and variance

$$\mathrm{Var}(\phi) = \frac{d}{L} s_\theta^2 + \mathcal{O}\left(\frac{s_\theta^3}{\theta_0^3}\right). \quad (6)$$

Thus $E[\phi]$ is given by θ_0, with the addition of a random walklike drift term proportional to s_θ^2. In addition, $\mathrm{Var}(\phi)$

increases with s_θ^2, but increasing the boundary length suppresses it as $1/L$. In the limit $L \to \infty$ reflection is thus completely specular, with a fixed scattering phase ϕ. This algebraic decay of diffusive scattering resembles a classical optical mirror [2].

If $\theta_0 = 0$, surprisingly there is no suppression of $\mathrm{Var}(\phi)$ with L. Rather, we find [27] that $\tan\phi$ follows a Cauchy distribution $f(\tan\phi) = \gamma/\pi(\tan^2\phi + \gamma^2)$ with $E[\phi] = 0$, $\mathrm{Var}(\phi) \approx 2.2 s_\theta$ linear in s_θ instead of quadratic, and $\gamma \approx 0.8 s_\theta$ obtained numerically. In this case, the law of reflection therefore breaks down and scattering is always diffusive. The distribution of the scattering phase follows the Cauchy distribution also when the disorder is non-Gaussian and even asymmetric, as long as θ_0 is sufficiently small. For an asymmetric distribution, the value of γ/s_θ weakly depends on higher cumulants of the distribution of $\theta(x)$.

Generic graphene boundaries support bands of edge states with a linear dispersion [23,26]. Because the matrix element between the edge state and the edge disorder is inversely proportional to the spatial extent of the edge state, the disorder broadening of these edge states is proportional to the momentum along the boundary [see Figs. 2(c), 2(d)]. In other words, linearly dispersing edge states turn into disorder-broadened bands with both the average velocity and the bandwidth proportional to $k_\parallel$. When these bands overlap with $E = 0$ they serve as a source of resonant scattering responsible for the breakdown of the law of reflection. Indeed, we find that the condition for diffusive scattering occurs for any $\theta_0 \lesssim s_\theta$.

To include intervalley scattering, we compute the scattering phase at the charge neutrality point using the nearest neighbor tight-binding model of graphene, with random on-site disorder in the outermost row of atoms taken from a Gaussian distribution with mean V_d and variance s_d^2 [27]. The results, shown in Fig. 2(b), agree with the single valley prediction of the Dirac equation up to numerical prefactors.

To extend our analysis to nonzero E_F, we employ the tight-binding model with on-site disorder to study the reflection angle φ at the disordered boundary numerically using Kwant [28]. The disordered edge band now resides at the energy V_d, as Figs. 2(c) and 2(d) show. Figures 2(a), 2(b) confirm that $\sigma^2(\varphi) \approx \mathrm{Var}(\phi)$ at $E = 0$. The law of reflection is broken for all s_d at $V_d = E_F$ and $\mathrm{Var}(\phi)$ increases linearly with s_d, independent of λ_F. Further, the reflection becomes specular for $s_d \lesssim |V_d - E_F|$. As Fig. 2(b) shows, $\mathrm{Var}(\phi)$ $[\sigma^2(\varphi)]$ increases quadratically with the disorder strength s_d, but decays as $1/L$ $[1/\lambda_F]$ [Fig. 2(a)] when the Fermi wavelength becomes large compared to the lattice constant a, such that scattering is predominantly specular. However, for $s_d \gtrsim |V_d - E_F|$ reflection becomes diffusive, and moving V_d closer to E_F [Fig. 2(b)] shifts the transition from specular to diffusive reflection to smaller s_d.

Experimental detection.—Any experiment that is sensitive to the microscopic properties of a disordered boundary will detect the breakdown of the law of reflection if the disordered edge band overlaps with the Fermi level. We propose to search for a transport signature of the breakdown of the law of reflection in the magnetic focusing experiment sketched in Fig. 1. The idea is to study the

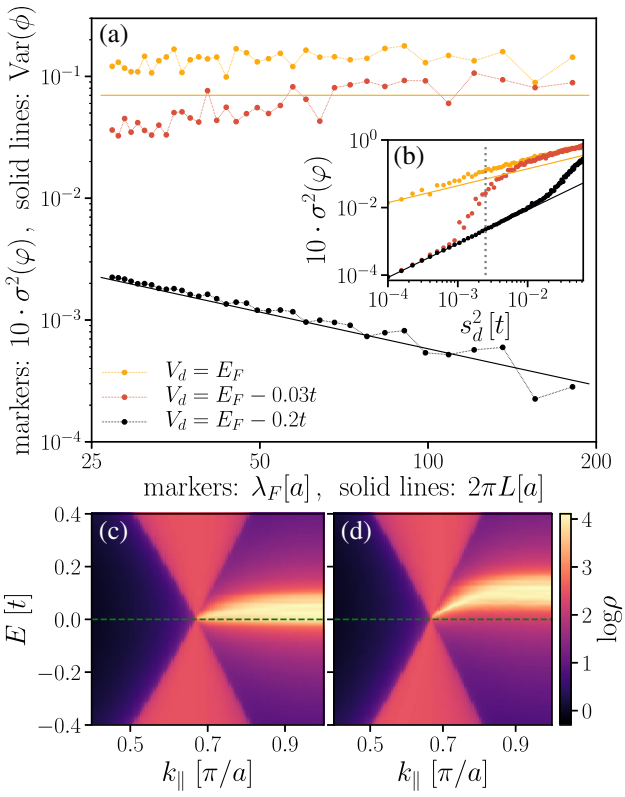

FIG. 2. (a) Solid lines: $\mathrm{Var}(\phi)$ at the Dirac points ($E_F = 0$) as a function of the boundary length L, for a disorder strength $s_d = 0.05t$ obtained from the tight-binding model. Markers: $\sigma^2(\varphi)$ at finite E_F, averaged over all incoming modes and 10^2 disorder configurations, as a function of the Fermi wavelength λ_F for the same disorder strength, obtained numerically for a semi-infinite graphene sheet with a boundary of length $L = 300a$. The values chosen for $\lambda_F = \sqrt{3}\pi t a/E_F$ correspond to E_F ranging from $0.2t$ to $0.03t$. (b) Same as (a), as a function of the disorder strength s_d^2, for a value of $2\pi L \approx 27a$ [$\lambda_F \approx 27a$, $E_F = 0.2t$]. The dotted line indicates the value of s_d used in (a). For $V_d = E_F$ the variances of both the scattering phase at $E_F = 0$ and the reflection angle at $E_F > 0$ increase linearly with s_d, independent of the Fermi wavelength, exhibiting the breakdown of the law of reflection. For $|V_d - E_F| \gtrsim s_d$, $\mathrm{Var}(\phi)$ $[\sigma^2(\varphi)]$ decays with increasing L $[\lambda_F]$ as $1/L$ $[1/\lambda_F]$ and increases quadratically with the disorder strength [as given by Eq. (6)]. Reflection is thus specular, but becomes diffusive for $|V_d - E_F| \lesssim s_d$. Setting V_d closer to E_F moves transition between the regimes of specular and diffusive reflection to smaller s_d. This is because of the overlap of E_F with the disorder-broadened edge band. (c),(d) Momentum-resolved density of states at the disordered zigzag edge of a semi-infinite graphene sheet with a boundary of length $L = 300a$. A band of edge states with bandwidth $\propto s_d = 0.05t$ extends between the Dirac cones, residing mostly at energy V_d, with $V_d = 0.03t$ in (c) and $V_d = 0.2t$ in (d) [dashed lines].

reflection of ballistic cyclotron trajectories in a magnetic field B off a graphene edge [9,14,15]. The use of a collimator could improve such an experiment [16].

Magnetic focusing refers to the appearance of peaks in the nonlocal conductance between the source and the drain when a voltage is applied between the source and the grounded ribbon, cf. Fig. 1. There is an increased probability for electrons to end up in the drain whenever the separation W_x between source and drain matches an integer multiple of the cyclotron diameter $2r_c$, where $r_c = \hbar k_F/eB$ is the cyclotron radius with k_F the Fermi momentum, $\hbar$ the reduced Planck constant, and e the elementary charge. Because of the linear dispersion near the charge neutrality point in graphene, $k_F = E_F/\hbar v_F$ is linear in E_F, such that focusing peaks appear at the magnetic fields $B_n^f = 2nE_F/ev_F W_x$, $n \in \mathbb{N}$. For the setup in Fig. 1 but with a clean, specularly reflecting system edge, Fig. 3(a) shows a map of the first few focusing conductance peaks with their predicted locations marked. At resonance p, the electron beam reflects specularly $p-1$ times at the system edge before exiting into the drain, as Fig. 1 demonstrates for $p = 2$. On the other hand, if reflection from the boundary is diffusive, the electrons scatter into random angles off the boundary, which in general no longer result in cyclotron trajectories that are commensurate with the distance from the focus point at the boundary to the drain. In comparison with the case of specular reflection, the focusing beam at the drain is therefore diminished for diffusive edge scattering, resulting in a drop in the $p > 1$ conductance resonances. Because the reflection is diffusive when the disordered edge band overlaps with the Fermi level, by using a side gate (see Fig. 1) to tune the average potential at the disordered boundary, it is therefore possible to observe signatures of the breakdown of the law of reflection in the form of a conductance drop at a focusing peak.

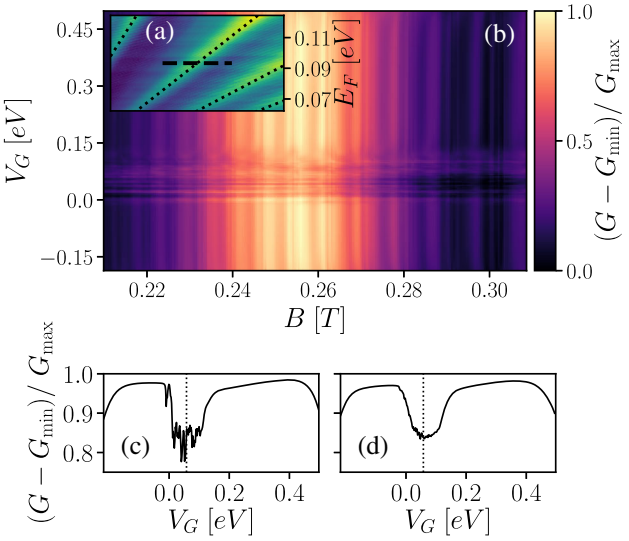

FIG. 3. (a) Conductance as a function of Fermi energy and magnetic field showing the first 4 magnetic focusing peaks for the device sketched in Fig. 1 in the absence of edge disorder and with $V_G = 0$. Superimposed are the predicted locations of the focusing peaks (dotted lines), $1 \le p \le 4$ from left to right across the diagonal. The color scale is linear and ranges from about $4e^2/h$ (dark) to $28e^2/h$ (bright). (b) Conductance around the $p = 2$ focusing peak at $E_F = 0.093$ eV [dashed line in (a)] versus gate voltage. We include disorder with $V_d = 0.062$ and $s_d = 0.047$ eV in the first $N = 6$ rows next to the boundary. Reflection at the boundary is specular and the conductance smooth in V_G, except for a dip when the disordered edge band overlaps with the Fermi level, and reflection becomes diffusive. (c) Line cut from (b) at $B = 0.256$ T with the predicted voltage value for the dip marked. Within the dip, the conductance exhibits fluctuations dependent on the particular disorder configuration, that are washed out by disorder averaging in (d). We assume the scaling factor $s = 9$ in the tight-binding model, such that $W_x = 1.6$, $W_y = 1$, and $W_L = 0.2$ μm.

To verify our prediction, we perform numerical simulations of the graphene focusing device with a side gate sketched in Fig. 1. We implement the tight-binding model for graphene in Kwant [28] and include the magnetic field via a Peierls substitution. We apply a random uniformly distributed on-site potential with mean V_d and variance s_d^2 to the first several rows of atoms adjacent to the system edge. We simulate the effect of a side gate by applying an extra potential with amplitude V_G exponentially decaying away from the sample edge on a length scale comparable to the size of the disordered region. Away from the charge neutrality point, we expect peak diffusive edge scattering to occur when the average potential by the boundary matches the Fermi energy. The relevant scales for our simulations are the hopping t, the graphene lattice constant $a = 2.46$ Å, and the magnetic flux $\Phi \propto Ba^2$ per unit cell. Scaling the tight-binding Hamiltonian with a scaling factor s [29] by reinterpreting $t/s \equiv t$, $sa \equiv a$ and $B/s^2 \equiv B$ such that Φ is unchanged by the scaling, our simulations apply to graphene devices of realistic and experimentally realizable dimensions [14,15]. Note that the on-site disorder correlation length is not scale invariant, and the disorder thus correlates s lattice sites in the original model.

Tuning the average potential at the disordered system edge by varying the side gate V_G reveals a clear dip in the conductance Fig. 3(b) around the second focusing resonance $p = 2$, which is absent when no edge disorder is included [27]. Outside the dip the conductance only changes weakly with V_G, which is the expected behavior for a clean specularly reflecting boundary. Here, the first $N = 6$ rows of sites adjacent to the edge are disordered, and the extent of the disordered region into the graphene sheet thus approximately $2.1a \ll \lambda_F \approx 18a$, such that the length scales are consistent with specular reflection. The conductance fluctuates erratically within the dip, as the line cut Fig. 3(c) taken from Fig. 3(b) at $B = 0.256$ T shows. These are universal conductance oscillations particular to an individual disorder configuration. They are washed out by disorder averaging as Fig. 3(d) shows, revealing an

omnipresent conductance dip. Furthermore, the conductance dip appears when the disordered edge band overlaps with E_F, which is the condition for the breakdown of the law of reflection, with the V_G that aligns the band with E_F marked in Figs. 3(c) and 3(d).

Conclusion and discussion.—Our analysis of scattering at a disordered graphene boundary reveals a regime where specular reflection is suppressed in favor of diffusive scattering. This counterintuitive conclusion holds even when conventional wisdom dictates that specular reflection should dominate and the boundary should act as a mirror, namely, when a boundary is rough on a length scale smaller than the Fermi wavelength. The origin of this breakdown of the law of reflection is resonant scattering of the electron waves from a linear superposition of localized boundary states. Our calculations show that this phenomenon is detectable in transverse magnetic focusing experiments, by employing a side gate to tune the average potential at the boundary. In these experiments the breakdown of specular reflection manifests as a dip in the nonlocal conductance at the second focusing resonance. Because the zigzag boundary condition is generic in graphene, we expect our results to apply to an arbitrary termination direction, and to be insensitive to microscopic details. We are thus confident that this effect is experimentally observable in present-day devices.

This work was supported by ERC Starting Grant No. 638760, the Netherlands Organisation for Scientific Research (NWO/OCW), and the U.S. Office of Naval Research.

*elias.walter@rwth-aachen.de
†torosdahl@gmail.com

[1] H. Davies, Proc. Inst. Elec. Eng. IV **101**, 209 (1954).
[2] H. E. Bennett and J. O. Porteus, J. Opt. Soc. Am. **51**, 123 (1961).
[3] A. K. Geim and K. S. Novoselov, Nat. Mater. **6**, 183 (2007).
[4] A. H. C. Neto, F. Guinea, N. M. R. Peres, K. S. Novoselov, and A. K. Geim, Rev. Mod. Phys. **81**, 109 (2009).
[5] C. H. Lui, L. Liu, K. F. Mak, G. W. Flynn, and T. F. Heinz, Nature (London) **462**, 339 (2009).
[6] C. R. Dean, A. F. Young, I. Meric, C. Lee, L. Wang, S. Sorgenfrei, K. Watanabe, T. Taniguchi, P. Kim, K. L. Shepard, and J. Hone, Nat. Nanotechnol. **5**, 722 (2010).
[7] A. S. Mayorov, R. V. Gorbachev, S. V. Morozov, L. Britnell, R. Jalil, L. A. Ponomarenko, P. Blake, K. S. Novoselov, K. Watanabe, T. Taniguchi, and A. K. Geim, Nano Lett. **11**, 2396 (2011).
[8] L. Banszerus, M. Schmitz, S. Engels, M. Goldsche, K. Watanabe, T. Taniguchi, B. Beschoten, and C. Stampfer, Nano Lett. **16**, 1387 (2016).
[9] H. van Houten and C. Beenakker, Quantum Point Contacts and Coherent Electron Focusing, in *Analogies in Optics and Micro Electronics*, edited by W. van Haeringen and D. Lenstra (Kluwer, Dordrecht, 1990).
[10] V. V. Cheianov, V. Fal'ko, and B. L. Altshuler, Science **315**, 1252 (2007).
[11] S. Chen, Z. Han, M. M. Elahi, K. M. M. Habib, L. Wang, B. Wen, Y. Gao, T. Taniguchi, K. Watanabe, J. Hone, A. W. Ghosh, and C. R. Dean, Science **353**, 1522 (2016).
[12] P. Rickhaus, P. Makk, M.-H. Liu, E. Tóvári, M. Weiss, R. Maurand, K. Richter, and C. Schönenberger, Nat. Commun. **6**, 6470 (2015).
[13] T. Taychatanapat, J. Y. Tan, Y. Yeo, K. Watanabe, T. Taniguchi, and B. Özyilmaz, Nat. Commun. **6**, 6093 (2015).
[14] T. Taychatanapat, K. Watanabe, T. Taniguchi, and P. Jarillo-Herrero, Nat. Phys. **9**, 225 (2013).
[15] S. Bhandari, G.-H. Lee, A. Klales, K. Watanabe, T. Taniguchi, E. Heller, P. Kim, and R. M. Westervelt, Nano Lett. **16**, 1690 (2016).
[16] A. W. Barnard, A. Hughes, A. L. Sharpe, K. Watanabe, T. Taniguchi, and D. Goldhaber-Gordon, Nat. Commun. **8**, 15418 EP (2017).
[17] Y.-W. Son, M. L. Cohen, and S. G. Louie, Phys. Rev. Lett. **97**, 216803 (2006).
[18] D. Halbertal, M. Ben Shalom, A. Uri, K. Bagani, A. Y. Meltzer, I. Marcus, Y. Myasoedov, J. Birkbeck, L. S. Levitov, A. K. Geim, and E. Zeldov, Science **358**, 1303 (2017).
[19] D. A. Areshkin, D. Gunlycke, and C. T. White, Nano Lett. **7**, 204 (2007).
[20] M. Evaldsson, I. V. Zozoulenko, H. Xu, and T. Heinzel, Phys. Rev. B **78**, 161407 (2008).
[21] S. Masubuchi, K. Iguchi, T. Yamaguchi, M. Onuki, M. Arai, K. Watanabe, T. Taniguchi, and T. Machida, Phys. Rev. Lett. **109**, 036601 (2012).
[22] V. K. Dugaev and M. I. Katsnelson, Phys. Rev. B **88**, 235432 (2013).
[23] A. R. Akhmerov and C. W. J. Beenakker, Phys. Rev. B **77**, 085423 (2008).
[24] M. V. Berry and R. J. Mondragon, Proc. R. Soc. A **412**, 53 (1987).
[25] E. McCann and V. I. Fal'ko, J. Phys. Condens. Matter **16**, 2371 (2004).
[26] J. A. M. van Ostaay, A. R. Akhmerov, C. W. J. Beenakker, and M. Wimmer, Phys. Rev. B **84**, 195434 (2011).
[27] See Supplemental Material at http://link.aps.org/supplemental/10.1103/PhysRevLett.121.136803 for details on the analytical derivation and additional numerical data, as well as the code for the numerical simulations.
[28] C. W. Groth, M. Wimmer, A. R. Akhmerov, and X. Waintal, New J. Phys. **16**, 063065 (2014).
[29] M.-H. Liu, P. Rickhaus, P. Makk, E. Tóvári, R. Maurand, F. Tkatschenko, M. Weiss, C. Schönenberger, and K. Richter, Phys. Rev. Lett. **114**, 036601 (2015).